Applied Thermal Engineering 51 (2013) 753–763

Contents lists available at SciVerse ScienceDirect

Applied Thermal Engineering

journal homepage: www.elsevier.com/locate/apthermeng

Decentralized optimization for vapor compression refrigeration cycle

Lei Zhao, Wen-Jian Cai*, Xu-dong Ding, Wei-chung Chang

Centre for E-City, School of Electrical and Electronic Engineering, Nanyang Technological University, BLK S2-B2a-08, Nanyang Ave, Singapore 639798, Singapore

HIGHLIGHTS

► The decentralized optimization problem of VCC is formulated.
► Decentralized optimization technique is modified and applied to the problem.
► Experiments show proposed method energy consumption is close to global optimization.
► Experiments show proposed method is much faster than global optimization.

ARTICLE INFO

Article history:
Received 22 May 2012
Accepted 3 October 2012
Available online 12 October 2012

Keywords:
Vapor compression refrigeration cycle
Hybrid component models
Decentralized problem formulation
Decentralized optimization

ABSTRACT

This paper presents a model based decentralized optimization method for vapor compression refrigeration cycle (VCC). The overall system optimization problem is formulated and separated into minimizing the energy consumption of three interactive individual subsystems subject to the constraints of hybrid model, mechanical limitations, component interactions, environment conditions and cooling load demands. Decentralized optimization method from game theory is modified and applied to VCC optimization to obtain the Perato optimal solution under different working conditions. Simulation and experiment results comparing with traditional on–off control and genetic algorithm are provided to show the satisfactory prediction accuracy and practical energy saving effect of the proposed method. For the working hours, its computation time is steeply reduced to 1% of global optimization algorithm with consuming only 1.05% more energy consumption.

1. Introduction

The refrigeration industry was firstly evolved in response to the pressing need to preserve and transport food for expanding populations. It continued to grow as human comfort and industrial applications demands. Its applications can be divided into four groups: food production and distribution, chemical and industry processes, special application and comfort air conditioning [1]. The energy consumption of refrigeration system is quite large in industry as well as domestic usage. For instance, statistical data shows air conditioner and refrigerator account for 28% of home energy consumption in US [2]. For hot and humid tropical country such as Singapore, this ratio can even rise to over 50% [3]. Among all types of cooling systems, electricity based vapor compression cooling systems are still dominant in the current market. The effort to reduce the energy consumption through system control and optimization in vapor compression refrigeration system is of practical significance due to both energy shortage and global warming concerns [4].

During earlier studies, system optimization was based on experience and intuitive analysis because simple yet reliable model of each component was not established. Stoecker claimed that to increase heat exchanging efficiency so that to achieve higher Coefficient of Performance (COP), superheat and subcool should both be minimized [5]. With the introduction of variable speed drive to the compressor and electronic expansion valve, the energy saving potential of vapor compression cycle (VCC) was further studied, theoretical comparison of various refrigeration capacity control methods in full and part-load conditions shows that both of them are efficient technique for capacity control [6,7]. Optimization scheme for whole system based on components' polynomial models was also investigated, Sanaye et al. assigned cost functions for components and used Lagrange multipliers method to minimize the objective function [8]. Jensen and Skogestad proposed to add an active charger as complementary variable for manipulation and discussed the selection of the controlled variable to improve the system efficiency [9–11]. Larsen et al. proposed a gradient method to find the suboptimal solution for condensing pressure, while keep

* Corresponding author. Tel.: +65 6790 6862; fax: +65 6793 3318.
E-mail address: ewjcai@ntu.edu.sg (W.-J. Cai).

1359-4311/$ – see front matter © 2012 Elsevier Ltd. All rights reserved.
http://dx.doi.org/10.1016/j.applthermaleng.2012.10.001

Nomenclatures

A_v	opening percentage of electronic expansion valve
c	coefficients of hybrid models
d	coefficients of cost functions
f	function
F	frequency of compressor
K	penalty
H	enthalpy
$H_{c,fg}$	enthalpy difference of gas and liquid saturated refrigerant in condenser
$H_{c,r,i}$	condenser inlet refrigerant enthalpy
$H_{c,r,o}$	condenser outlet refrigerant enthalpy
$H_{com,r,i}$	compressor inlet refrigerant enthalpy
$H_{com,r,o}$	compressor outlet refrigerant enthalpy
$H_{e,g}$	enthalpy of saturated refrigerant in evaporator
$H_{e,r,i}$	evaporator inlet refrigerant enthalpy
$H_{e,r,o}$	evaporator outlet refrigerant enthalpy
$H_{i,s}$	compressor outlet refrigerant enthalpy under isentropic compression
H_k	Cholesky factorization of Hessian Matrix of the cost function in step k
M	Cholesky factorization of Hessian Matrix of the cost function
$\dot{m}_{c,air}$	air flow rate of condenser
$\dot{m}_{c,air,max}$	upper bound of air flow rate of condenser
$\dot{m}_{c,air,min}$	lower bound of air flow rate of condenser
$\dot{m}_{c,air,nom}$	nominal air flow rate of condenser
$\dot{m}_{e,air}$	air flow rate of evaporator
$\dot{m}_{e,air,max}$	upper bound of air flow rate of evaporator
$\dot{m}_{e,air,min}$	lower bound of air flow rate of evaporator
$\dot{m}_{e,air,nom}$	nominal air flow rate of evaporator
$\dot{m}_r$	refrigerant mass flow rate
$\dot{m}_{r,max}$	maximal refrigerant mass flow rate
$\dot{m}_{r,min}$	minimal refrigerant mass flow rate
P_c	refrigerant saturated pressure in condenser
$P_{c,max}$	maximal condenser saturated pressure allowed
$P_{c,min}$	minimal condenser saturated pressure allowed
P_e	refrigerant saturated pressure in evaporator
$P_{e,max}$	maximal evaporator saturated pressure allowed
$P_{e,min}$	minimal evaporator saturated pressure allowed
$\dot{Q}_c$	heat transfer rate in condenser
$\dot{Q}_e$	heat transfer rate in evaporator
$\dot{Q}_{com}$	heat transfer rate in compressor
$\dot{Q}_{req}$	cooling load requirement
$T_{c,air,i}$	condenser inlet air temperature
$T_{c,max}$	maximal refrigerant saturation temperature in condenser
$T_{c,min}$	minimum refrigerant saturation temperature in condenser
$T_{c,r,i}$	condenser inlet refrigerant temperature
$T_{c,r,o}$	condenser outlet refrigerant temperature
$T_{c,sc}$	condenser subcool temperature
$T_{c,r,sat}$	condenser refrigerant saturated temperature
$T_{com,r,i}$	compressor inlet refrigerant temperature
$T_{com,r,o}$	compressor outlet refrigerant temperature
$T_{e,air,i}$	evaporator inlet air temperature
$T_{e,r,i}$	evaporator refrigerant inlet temperature
$T_{e,r,o}$	evaporator refrigerant outlet temperature
$T_{e,r,sat}$	refrigerant saturated temperature in evaporator
$T_{e,max}$	maximal refrigerant saturation temperature in evaporator
$T_{e,min}$	minimal refrigerant saturation temperature in evaporator
$T_{e,sh}$	evaporator superheat temperature
$T_{e,max}$	upper bound of superheat
$T_{e,min}$	lower bound of superheat
$\dot{W}_{c,fan}$	condenser fan power
$\dot{W}_{c,fan,nom}$	condenser fan power when air flow rate is $m_{c,air,nom}$
$\dot{W}_{com}$	electricity power consumption of compressor
$\dot{W}_{c,fan}$	evaporator fan power
$\dot{W}_{e,fan,nom}$	evaporator fan power when air flow rate is $m_{e,air,nom}$
$\dot{W}_{total}$	total power
x	state vector of subsystem
η_{com}	enthalpy delivery efficiency of compressor
ρ	inlet refrigerant density
β	coefficients of energy consumption terms
γ	updating coefficient of β

Subscripts

air	feature of air
c	condenser
com	compressor
e	evaporator
ev	expansion valve
fan	evaporator or condenser fan
i	inlet
k	number of current cycle
m	mass flow rate
r	refrigerant
o	outlet
η	enthalpy delivery efficiency

the superheat and evaporating pressure constant [12]. Recently, Barreira et al. optimized the split type residential air conditioner based on thermoeconomic analysis [13]. Zhou et al. employed theoretical model of air conditioning cycle components, formulated and solved a multi-objective optimization problem for high heat flux removal [14].

Unfortunately, few research papers have been published through the view of systematic optimization of VCC, because components of vapor compression refrigeration cycle are severely interacted, these interactions complicate the optimization problem as well as the solving procedures. The optimization problem discussed in similar system (HVAC) includes the work of Kusiak et al. They proposed series of data driven system optimization techniques for commercial HVAC systems. Simulation results based on experiment conducted showed that system level optimization can improve overall system operating performance significantly [15–17]. Fong et al. utilized robust evolutionary method to obtain appropriate energy management measure for HVAC system [18]. Ning proposed a neural network based optimal supervisory operation strategy to find the optimal set points [19]. To minimize HVAC system energy consumption, Yao et al. developed a global optimization model based on decomposition–coordination algorithm [20].

Although these methods have been proved effective, the computation burden of the existed algorithm based on centralized formulation is too large for online optimization. The convergence time, though can be neglected in academic research, is an important factor in practice. Recently, a relatively novel optimization method called decentralized optimization has been proposed in Refs. [21,22] by Inalhan. In the decentralized optimization algorithm, the original problem can be separated into several subsystem optimizations with constraints updating. It has been proved that decentralized optimization can converge to Nash Equilibrium of the original problem with much higher speed and lower computation burden. Therefore, decentralized optimization is a promising alternative to balance minimizing energy consumption and converging speed.

In this paper, we applied the decentralized optimization algorithm to the VCC by 1) decompose the complex global optimization problem of VCC into evaporator, condenser and compressor optimization subproblems based on component hybrid models and interactive constraints; 2) propose a modified decentralized optimization method to simplify the original problem by transforming it into unconstrained subsystem optimization problems so that gradient based search methods can then be easily applied to each subsystem. Simulation and experimental results on a lab scale pilot plant demonstrate that the performance of the proposed decentralized optimization method is comparable to that of centralized optimization method. However, the reduction in computation time is on the scale of 100 times.

2. Working principle and component models

The vapor compression cycle has basically four components – Evaporator, Compressor, Condenser, and Expansion Valve, as shown in Fig. 1. These four components are connected in a closed loop so that the working fluid is continuously circulated in the cycle. Its working principle is briefly stated below:

1. Starting from the evaporator side of the cycle; the temperature T inside the evaporator is lower than the cold reservoir temperature $T_{e,air,i}$, which results in heat being transferred from the cold reservoir to the refrigerant.
2. The ensuing high temperature refrigerant is compressed by the compressor as a high temperature and high pressure vapor.
3. In the condenser, the high temperature and high pressure vapor gives away its heat to the outside environment (hot reservoir).
4. This condensed liquid refrigerant is then passed through the expansion valve which drastically reduces the pressure of refrigerant from condensing pressure P_c to evaporating pressure P_e. The reduction in pressure also reduces the temperature of refrigerant in the evaporator, thus the low pressure and low temperature refrigerant enters the evaporator to continue the cycle (Fig. 2).

The mathematical models of the four components which indicate the transition of the refrigerant between the states are instrumental in the model based optimization, they are given below:

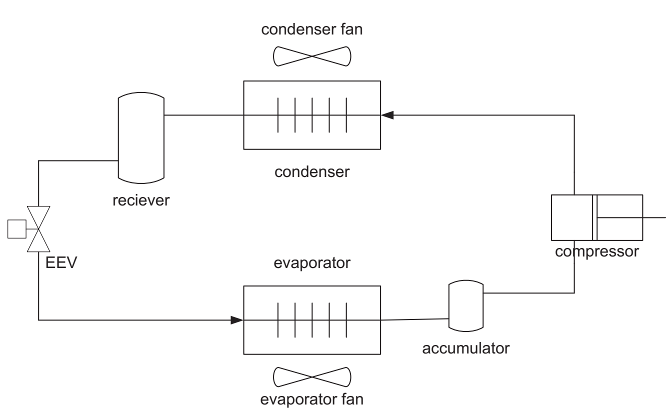

Fig. 1. Vapor compression refrigeration cycle.

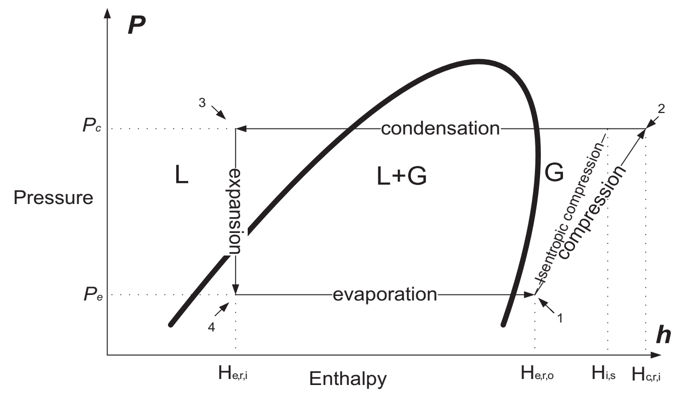

Fig. 2. P–h chart of vapor compression cycle.

2.1. Evaporator

According to energy balance equation, energy absorbed by the refrigerant is equal to energy reduction in the cold reservoir [23], i.e.

$$\dot{Q}_e = \dot{m}_r (H_{e,r,o} - H_{e,r,i}) \tag{1}$$

where $\dot{Q}_e$, $\dot{m}_r$, $H_{e,r,i}$ and $H_{e,r,o}$ are heat transfer rate in evaporator, mass flow rate of refrigerant, refrigerant enthalpy at evaporator inlet and outlet, respectively (see Appendix A for the calculation of $H_{e,r,i}$ and $H_{e,r,o}$).

The energy absorbed by the refrigerant can also be obtained from the hybrid model which reveals heat transfer property between refrigerant and air [24]:

$$\dot{Q}_e = \frac{(H_{e,g} - H_{e,r,i})\dot{m}_r + c_{e,1}\dot{m}_r^{c_{e,3}}(T_{e,air,i} - T_{e,r,sat})}{1 + c_{e,2}\left(\frac{\dot{m}_r}{\dot{m}_{e,air}}\right)^{c_{e,3}}} \tag{2}$$

where $c_{e,1}$,$c_{e,2}$ and $c_{e,3}$ are constants obtained by experiment data, $H_{e,g}$, $\dot{m}_{e,air}$, $T_{e,air,i}$ and $T_{e,r,sat}$ are the enthalpy of saturated gas phase refrigerant in evaporator, air outside evaporator, temperature of inlet air and saturated refrigerant of evaporator, respectively (see Appendix A for the calculations of $H_{e,g}$ and $T_{e,r,sat}$).

Furthermore, several physical constraints are imposed to restrict the state variables for proper operation of evaporator, including:

1. Evaporator air mass flow rate: determined by characteristic of evaporator fan

$$\dot{m}_{e,air,min} \le \dot{m}_{e,air} \le \dot{m}_{e,air,max} \tag{3}$$

where $\dot{m}_{e,air,min}$ and $\dot{m}_{e,air,max}$ are the lower and upper bounds of evaporator air mass flow rate, respectively.

2. Evaporating temperature: the heat absorption in evaporator results the increase of refrigerant temperature [25]

$$T_{e,r,i} \le T_{e,r,sat} \le T_{e,r,o} \tag{4}$$

where $T_{e,r,i}$ and $T_{e,r,o}$ are refrigerant temperature at evaporator inlet and outlet.

3. Superheat: superheat temperature which is defined as outlet refrigerant temperature minus saturated temperature, if too

low, will cause hunting in the cycle [26]. On the other hand, the COP of system will decrease steeply if the superheat temperature is too high [5,27].

$$T_{e,sh,min} \le T_{e,sh} \le T_{e,sh,max} \tag{5}$$

where $T_{e,sh,min}$ and $T_{e,sh,max}$ are lower and upper bounds of superheat which depend on the system configurations.

2.2. Condenser

The corresponding energy balance equation is as follows [23]:

$$\dot{Q}_c = \dot{m}_r(H_{c,r,i} - H_{c,r,o}) \tag{6}$$

where $\dot{Q}_c$, $H_{c,r,i}$ and $H_{c,r,o}$ are the heat transfer rate of condenser, enthalpy of inlet and outlet refrigerant in condenser, respectively (see Appendix A for the calculations of $H_{c,r,i}$ and $H_{c,r,o}$).

While the energy discharged by the refrigerant can also be obtained from the hybrid model [28]:

$$\dot{Q}_c = \frac{c_{c,1}\dot{m}_r^{c_{c,4}}(T_{c,r,sat} - T_{c,air,i}) + c_{c,2}\dot{m}_r(T_{c,r,i} - T_{c,r,sat}) + H_{c,fg}\dot{m}_r}{1 + c_{c,3}\left(\dfrac{\dot{m}_r}{\dot{m}_{c,air}}\right)^{c_{c,4}}} \tag{7}$$

where $c_{c,1}$,$c_{c,2}$, $c_{c,3}$ and $c_{c,4}$ are constants calculated through fitting experiment data, $H_{c,fg}$ is enthalpy difference between saturated liquid and gas phase refrigerant in condenser, $\dot{m}_{c,air}$ is the mass flow rate of air outside condenser. $T_{c,r,sat}$, $T_{c,r,i}$, $T_{c,air,i}$ are temperatures of saturated refrigerant, inlet refrigerant and inlet air of condenser, respectively (see Appendix A for the calculations of $H_{c,fg}$ and $T_{c,r,sat}$).

Similar to evaporator, the physical constraints of state variables of the condensers are listed as follows:

1. Condenser air mass flow rate: similar to evaporator fan, condenser fan limits the maximal and minimal air mass flow rates

$$\dot{m}_{c,air,min} \le \dot{m}_{c,air} \le \dot{m}_{c,air,max} \tag{8}$$

where $\dot{m}_{c,air,min}$ and $\dot{m}_{c,air,max}$ are the lower and upper bounds of condenser air mass flow rate

2. Condensing temperature: as refrigerant rejects heat in condenser, the condensing temperature is lower than inlet refrigerant temperature while higher than outlet refrigerant temperature [25].

$$T_{c,r,o} \le T_{c,r,sat} \le T_{c,r,i} \tag{9}$$

3. Subcool: subcool ($T_{c,sc}$) is defined as refrigerant condensing temperature minus refrigerant temperature at condenser outlet, the working principle of air conditioner requires that subcool should not be negative [23], thus

$$T_{c,sc} \ge 0 \tag{10}$$

2.3. Compressor

According to energy balance equation, all of the heat generated by compressor is absorbed by refrigerant:

$$\dot{Q}_{com} = \dot{m}_r(H_{com,r,o} - H_{com,r,i}) \tag{11}$$

where $\dot{Q}_{com}$, $H_{com,r,i}$ and $H_{com,r,o}$ are heat transfer rate in compressor, enthalpy of inlet and outlet refrigerant in compressor, respectively (see Appendix A for the calculations of $H_{com,r,i}$ and $H_{com,r,o}$)

The hybrid models of heat transfer and mass flow rate of compressor are given below [29]

$$\dot{Q}_{com} = c_{com,q,1}F\dot{m}_rP_e\left(\left(\frac{P_c}{P_e}\right)^{c_{com,q,2}} - 1\right) \tag{12}$$

$$\dot{m}_r = \left(c_{com,m,1} - c_{com,m,2}\left(\frac{P_c}{P_e}\right)^{c_{com,m,3}}\right)F, \tag{13}$$

where $c_{com,m,1}$, $c_{com,m,2}$, $c_{com,m,3}$, $c_{com,q,1}$ and $c_{com,q,2}$ are constants determined by curve-fitting, P_c, P_e, F and Q_{com} are condensing pressure, evaporating pressure, compressor frequency, and heat rejected to refrigerant by compressor, respectively.

In addition, physical constraints of compressor are as following:

1. Compressor Frequency: the following physical constraint is directly determined by compressor working range.

$$F_{min} \le F \le F_{max} \tag{14}$$

2. Compressor refrigerant mass flow rate:

$$\dot{m}_{r,min} \le \dot{m}_r \le \dot{m}_{r,max} \tag{15}$$

where $\dot{m}_{r,min}$ and $\dot{m}_{r,max}$ are the minimal and maximal refrigerant mass flow rates of the system, both of which are determined by system characteristics.

3. Condensing and evaporating pressures in compressor: they are bounded for protecting compressor from being damaged

$$\begin{aligned} P_{c,min} &\le P_c \le P_{c,max} \\ P_{e,min} &\le P_e \le P_{e,max} \end{aligned} \tag{16}$$

where $P_{c,min}$, $P_{c,max}$, $P_{e,min}$ and $P_{e,max}$ are lower and upper bounds of condensing pressure (discharge pressure) and of evaporating pressure (suction pressure).

2.4. Expansion valve

The mass flow rate of expansion valve is determined by valve opening percentage, pressure difference and inlet refrigerant density. Its mass flow rate is given by Ref. [30]

$$\dot{m}_r = (c_{ev,1} + c_{ev,2}A_v)\sqrt{\rho(P_c - P_e)} \tag{17}$$

where $c_{ev,1}$ and $c_{ev,2}$ are constants, A_v and ρ are opening percentage of electronic expansion valve and density of inlet refrigerant, respectively (see Appendix A for the calculation of ρ). The inlet and outlet enthalpy should be equal, consequently refrigerant enthalpy is constant which implies $\dot{Q}_{ev} = 0$ [31].

Furthermore, the Opening Percentage of EEV is bounded as following:

$$0 < A_v \le 1 \tag{18}$$

3. Decentralized optimization problem formulation

In decentralized optimization, the whole refrigeration cycle is first separated into several loosely related subsystems, i.e.: evaporator, condenser and compressor due to their physical and geometrical independence. Moreover, EEV is integrated into compressor subsystem due to the similarity of their function upon controlling pressure and refrigerant mass flow rate. The interactions between the subsystems are defined as interactive constraints in the process of formulation.

3.1. Evaporator

The objective for isolated evaporator subsystem optimization would be minimizing evaporator fan energy consumption subject to cooling load requirement of cold reservoir, where the power consumption of evaporator fan is influenced by two parameters: mass flow rates of fluids and the pressure difference between the inlets and outlets can be described by Ref. [32]

$$\dot{W}_{\mathrm{e,fan}} = \dot{W}_{\mathrm{e,fan,nom}}\left(c_{\mathrm{e,fan},0} + c_{\mathrm{e,fan},1}\left(\frac{\dot{m}_{\mathrm{e,air}}}{\dot{m}_{\mathrm{e,air,nom}}}\right) + c_{\mathrm{e,fan},2}\left(\frac{\dot{m}_{\mathrm{e,air}}}{\dot{m}_{\mathrm{e,air,nom}}}\right)^2 + c_{\mathrm{e,fan},3}\left(\frac{\dot{m}_{\mathrm{e,air}}}{\dot{m}_{\mathrm{e,air,nom}}}\right)^3\right) \quad (19)$$

Since the three subsystems are closely coupled, other two subsystems will impose interactive constraints to the evaporator subsystem. These interactive constraints include:

1 Evaporator inlet refrigerant enthalpy: the analysis of EEV shows that the refrigerant enthalpy of evaporator inlet equals to that of condenser outlet

$$H_{\mathrm{e,r,i}} = H_{\mathrm{c,r,o}} \quad (20)$$

2 Evaporator outlet refrigerant temperature: since heat transfer in pipe is neglected, the refrigerant temperature at evaporator outlet should be equal to at compressor inlet

$$T_{\mathrm{e,r,o}} = T_{\mathrm{com,r,i}} \quad (21)$$

where $T_{\mathrm{com,r,i}}$ is refrigerant temperatures at compressor inlet.

3 Evaporating pressure: evaporating pressure in evaporator is the same as that in compressor

$$P_{\mathrm{e,e}} = P_{\mathrm{com,e}} \quad (22)$$

where $P_{\mathrm{e,e}}$ and $P_{\mathrm{com,e}}$ are evaporating and compressor inlet pressures, respectively.

By taking consideration of cooling load requirement, energy consumption, physical and interactive constraints, the decentralized optimization problem for the evaporator subsystem can be formulated into a penalty function with its objective function expressed as:

$$\textbf{Min}\quad C_{\mathrm{e}} = \beta_{\mathrm{e}}\dot{W}_{\mathrm{e,fan}} + d_{\mathrm{e},1}K_{\mathrm{e,i}} + d_{\mathrm{e},2}K_{\mathrm{e,o}} + d_{\mathrm{e},3}\left(\dot{Q}_{\mathrm{e}} - \dot{Q}_{\mathrm{req}}\right)^2 \quad (23)$$

where $d_{\mathrm{e},1}$, $d_{\mathrm{e},2}$ and $d_{\mathrm{e},3}$ are constant coefficients of penalty terms derived from constraints, β_{e}, is the coefficient of evaporator fan energy consumption; $K_{\mathrm{e,i}}$ and $K_{\mathrm{e,o}}$ are the terms of interactive and physical constraints on the penalty function, expressed by

$$K_{\mathrm{e,i}} = \left(T_{\mathrm{e,r,o}} - T_{\mathrm{com,r,i}}\right)^2 + \left(H_{\mathrm{e,r,i}} - H_{\mathrm{c,r,o}}\right)^2 + \left(P_{\mathrm{e,e}} - P_{\mathrm{com,e}}\right)^2 \quad (24)$$

and

$$K_{\mathrm{e,o}} = \frac{1}{\dot{m}_{\mathrm{e,air,max}}}\{\max[\max(\dot{m}_{\mathrm{e,air,min}} - \dot{m}_{\mathrm{e,air}}, 0), \max(\dot{m}_{\mathrm{e,air}} - \dot{m}_{\mathrm{e,air,max}}, 0)]\}^2 + \frac{1}{T_{\mathrm{e,max}}}\{\max[\max(T_{\mathrm{e,min}} - T_{\mathrm{e,r,sat}}, 0), \max(T_{\mathrm{e,r,sat}} - T_{\mathrm{e,max}}, 0)]\}^2 + \frac{1}{T_{\mathrm{e,sh,max}}}\{\max[\max(T_{\mathrm{e,sh,min}} - T_{\mathrm{e,sh}}, 0), \max(T_{\mathrm{e,sh}} - T_{\mathrm{e,sh,max}}, 0)]\}^2 \quad (25)$$

respectively.

3.2. Condenser

Similar to evaporator subsystem, the objective of decentralized optimization for condenser subsystem can be formulated minimizing the power consumption of condenser fan, which can be calculated through [32]

$$\dot{W}_{\mathrm{c,fan}} = \dot{W}_{\mathrm{c,fan,nom}}\left(c_{\mathrm{c,fan},0} + c_{\mathrm{c,fan},1}\left(\frac{\dot{m}_{\mathrm{c,air}}}{\dot{m}_{\mathrm{c,air,nom}}}\right) + c_{\mathrm{c,fan},2}\left(\frac{\dot{m}_{\mathrm{c,air}}}{\dot{m}_{\mathrm{c,air,nom}}}\right)^2 + c_{\mathrm{c,fan},3}\left(\frac{\dot{m}_{\mathrm{c,air}}}{\dot{m}_{\mathrm{c,air,nom}}}\right)^3\right) \quad (26)$$

The interactive constraints from the other two subsystems to the condenser subsystem include:

1 Condenser inlet refrigerant temperature: the refrigerant temperatures at condenser inlet ($T_{\mathrm{c,r,i}}$) and at compressor outlet ($T_{\mathrm{com,r,o}}$), are equal as the energy loss is negligible

$$T_{\mathrm{c,r,i}} = T_{\mathrm{com,r,o}} \quad (27)$$

2 Condenser outlet refrigerant enthalpy: the refrigerant enthalpies at condenser inlet and at compressor outlet are equal

$$H_{\mathrm{c,r,o}} = H_{\mathrm{e,r,i}} \quad (28)$$

3 Condensing pressure: condensing pressures in condenser, $P_{\mathrm{c,c}}$, and compressor, $P_{\mathrm{com,c}}$, (discharge pressure) should be equal.

$$P_{\mathrm{c,c}} = P_{\mathrm{com,c}} \quad (29)$$

Consequently, the simplified unconstraint optimization problem for condenser is formulated as

$$\textbf{Min}\quad C_{\mathrm{c}} = \beta_{\mathrm{c}}\dot{W}_{\mathrm{c,fan}} + d_{\mathrm{c},1}K_{\mathrm{c,i}} + d_{\mathrm{c},2}K_{\mathrm{c,o}} \quad (30)$$

where $d_{\mathrm{c},1}$ and $d_{\mathrm{c},2}$ are constant coefficients of penalty terms for violating interactive constraints and physical constraints of evaporator, respectively, β_{c} is the coefficient of energy consumption of condenser fan which gradually decrease during optimization.

$$K_{\mathrm{c,i}} = \left(T_{\mathrm{c,r,i}} - T_{\mathrm{com,r,o}}\right)^2 + \left(H_{\mathrm{c,r,o}} - H_{\mathrm{e,r,i}}\right)^2 + \left(P_{\mathrm{c,c}} - P_{\mathrm{com,c}}\right)^2 \quad (31)$$

and

$$K_{c,o} = \frac{1}{\dot{m}_{c,air,max}}\{\max[\max(\dot{m}_{c,air,min} - \dot{m}_{c,air}, 0), \max(\dot{m}_{c,air} - \dot{m}_{c,air,max}, 0)]\}^2 + \frac{1}{T_{c,max}}\{\max[\max(T_{c,min} - T_{c,r,sat}, 0), \max(T_{c,r,sat} - T_{c,max}, 0)]\}^2 + \{\max(-T_{e,sh}, 0)\}^2 \tag{32}$$

3.3. Compressor

The objective of decentralized optimization for compressor optimization is to minimize the power consumption of compressor, which is determined by [29]

$$\dot{W}_{com} = \frac{\dot{Q}_{com}}{\eta_{com}} \tag{33}$$

Using a hybrid model to describe the delivery coefficient of compressor, η_{com} [29]

$$\eta_{com} = c_{com,\eta,1} + c_{com,\eta,2}(P_c/P_e)^{c_{com,\eta,3}} \tag{34}$$

where $c_{com,\eta,1}$, $c_{com,\eta,2}$ and $c_{com,\eta,3}$ are constants calculated through fitting experiment data.

The interactive constraints from the other two subsystems to the compressor subsystem include:

$$\begin{cases} T_{com,r,o} = T_{c,r,i} \\ T_{com,r,i} = T_{e,r,o} \\ P_{com,c} = P_{c,c} \\ P_{com,e} = P_{e,e} \\ \dot{Q}_e = \dot{Q}_{e,req} \end{cases} \tag{35}$$

By combining of energy consumption, physical and interactive constraints, the decentralized optimization problem for the compressor subsystem can be formulated as:

$$\textbf{Min} \quad C_{com} = \beta_{com}\dot{W}_{com} + d_{com,1}K_{com,i} + d_{com,2}K_{com,o} \tag{36}$$

where $d_{com,1}$ and $d_{com,2}$ are coefficients of penalty terms for violating interactive constraints and physical constraints of compressor, respectively, β_{com} is a gradually decreasing coefficient of compressor energy consumption.

$$K_{com,i} = (T_{com,r,o} - T_{c,r,i})^2 + (T_{com,r,i} - T_{e,r,o})^2 + (P_{com,c} - P_{c,c})^2 + (P_{com,e} - P_{e,e})^2 + \left(\dot{Q}_e - \dot{Q}_{req}\right)^2 \tag{37}$$

and

$$K_{com,o} = \frac{1}{F_{max}}\{\max[\max(F_{min} - F, 0), \max(F - F_{max}, 0)]\}^2 + \frac{1}{\dot{m}_{r,max}}\{\max[\max(\dot{m}_{r,min} - \dot{m}_{com,r}, 0), \max(\dot{m}_{com,r} - \dot{m}_{r,max}, 0)]\}^2 + \frac{1}{P_{com,c,max}}\{\max[\max(P_{com,c,min} - P_{com,c}, 0), \max(P_{com,c} - P_{com,c,max}, 0)]\}^2 + \frac{1}{P_{com,e,max}}\{\max[\max(P_{com,e,min} - P_{com,e}, 0), \max(P_{com,e} - P_{com,e,max}, 0)]\}^2 + \{\max[\max(-A_v, 0), \max(A_v - 1, 0)]\}^2 \tag{38}$$

4. Decentralized optimization algorithm

A sequential optimization scheme is adopted in each optimization cycle, that is, for the results obtained from other two subsystems; the subsystem under optimization optimizes its own cost function with local selection of energy consumption coefficient, and sends the solution to other subsystems. Detailed procedures are given as following:

1. Coefficients initialization: For each subsystem, there are maximum four parameters, i.e., $d_{\cdot,1}$, $d_{\cdot,2}$, $d_{\cdot,3}$ and $\beta_{\cdot}$. Since violation of physical constraints cause damage to system, the corresponding coefficients $d_{\cdot,2}$ and $d_{\cdot,3}$ should have much larger values than that of $d_{\cdot,1}$ (in the factor of 5 is recommended), while $\beta_{\cdot}$ corresponding to the power consumption whose initial value should be 10 times larger than that of $d_{\cdot,2}$ or $d_{\cdot,3}$ to find the optimal solution without much consideration of other constraints at first.
2. Operating state initialization: The typical operation states will be used to initialize the states of the three subsystems.
3. Update: At each step, the states of all the subsystems are used to update interactive constraints. Then coefficients of energy consumption terms$\beta_{\cdot}$'s are updated by

$$\beta_{\cdot,k+1} = \gamma\beta_{\cdot,k} \quad 0 < \gamma < 1 \tag{39}$$

where γ is the updating coefficient.

4. Optimization: Line search Newton's method with Hessian modification is used to find the optimal states by [33]

$$x_{k+1} = x_k - \alpha_k M_k^{-1}\nabla f_k \tag{40}$$

where α_k, x_k, M_k and ∇f_k are the step length, state vector to be optimized, Cholesky factorization of Hessian Matrix (see Appendix C for its procedure) of the cost function and gradient vector of cost function, respectively.

5 Termination: the optimization will be terminated if: 1) the coefficients $\beta_{\cdot}$ of energy consumption terms in cost function is smaller than a predefined value ε (say 10^{-5}); or 2) the maximum number of predetermined generations is reached. Otherwise, return to step 3.

Remark 1. The choice of the parameter γ is a trade-off between the number of steps in each cycle and total number of cycles required. If γ is large, the coefficients $\beta_{\cdot}$ only decrease slightly, leading to small number of Newton steps for current cycle. On the other hand, if γ is small, bigger reduction will result $\beta_{\cdot}$ after each cycle. The converged point from last cycle may not be a good starting point for the current one; much more computation load of Newton method is expected in each cycle. The recommended value of γ is in between 0.1 and 0.3 [34].

Remark 2. The choice of α_k is to result a big cost function reduction in each cycle yet to keep the procedure simple. Here line search algorithm is utilized to try a series of potential candidates of α_k until the Wolfe conditions are satisfied (see Appendix B for details).

Remark 3. Different from the standard Newton method, modified Cholesky factorization rather than the original form of Hessian matrix is used in this work to ensure the search resulting in a lower cost. Moreover, contrast with Cholesky factorization, the modified

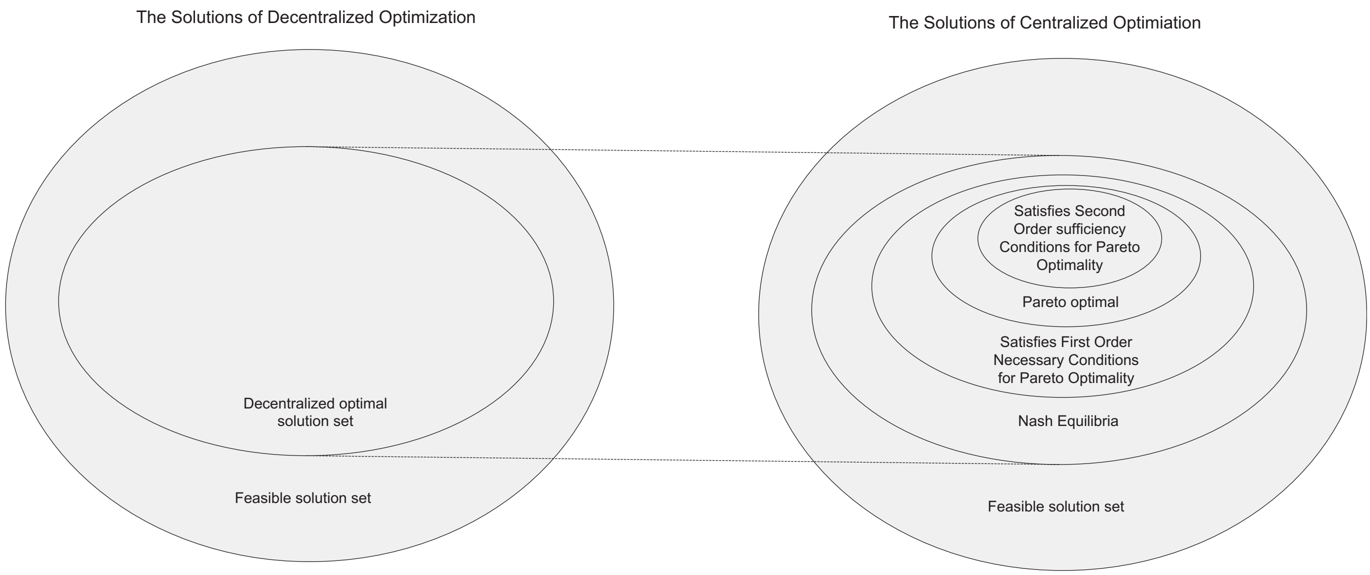

Fig. 3. Relations between decentralized and centralized optimal solutions.

form guarantees the existence and bound of Cholesky factors (see Appendix C for details) [33].

In summary, the outline of original decentralized optimization proposed by Inalhan is as follows [22,35]:

1. Separate the system to several subsystems
2. Formulate the objective function and constraints of each subsystem.
3. Each subsystem searches its own optimal solution under the constraints.
4. If subsystem B has a constraint involving subsystem A, update this constraint according to the value of A's optimal solution as soon as A finishes its optimization.
5. Stop if the predetermined termination criterion is met, otherwise go back to step 4.

The relation between solutions for centralized and decentralized optimization problems was given by Inalhan [21,35]:

1. Decentralized and centralized optimization have identical feasible solutions;
2. Decentralized optimal solutions equivalent to the Nash equilibrium of the global optimization problem.

Since VCC has numerous feasible operating states, there exists a set of feasible solutions which can be classified as the decentralized optimization solution set if they meet the constraint conditions, as shown in the left side circle of Fig. 3.

Table 1
Physical limits of variables.

Variables	Lower bound	Upper bound
$F_{c,fan}$	15 Hz	35 Hz
$F_{e,fan}$	15 Hz	30 Hz
$T_{c,r,sat}$	$T_{c,air,i}$	$T_{c,r,i}$
$T_{e,r,sat}$	12 °C	$T_{e,air,i}$
P_c	8 bar	15 bar
P_e	2 bar	5 bar
$T_{e,sh}$	5 °C	25 °C
$T_{c,sc}$	0 °C	NA
F_{com}	30 Hz	50 Hz
$\dot{m}_r$	0.008 kg/s	0.03 kg/s

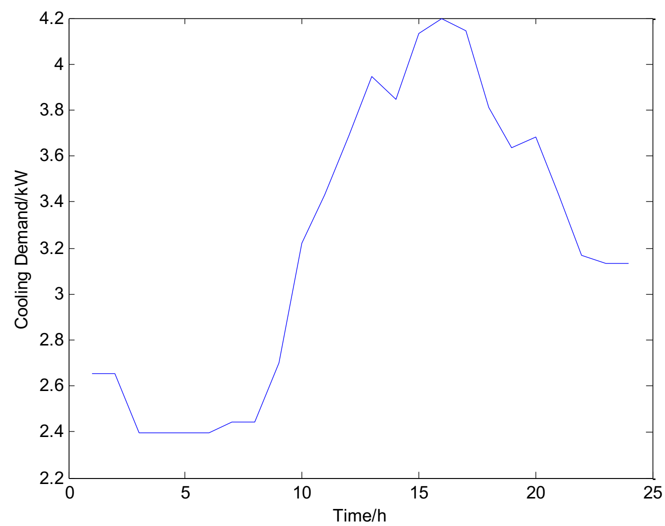

Fig. 4. Sample cooling load of Singapore [37].

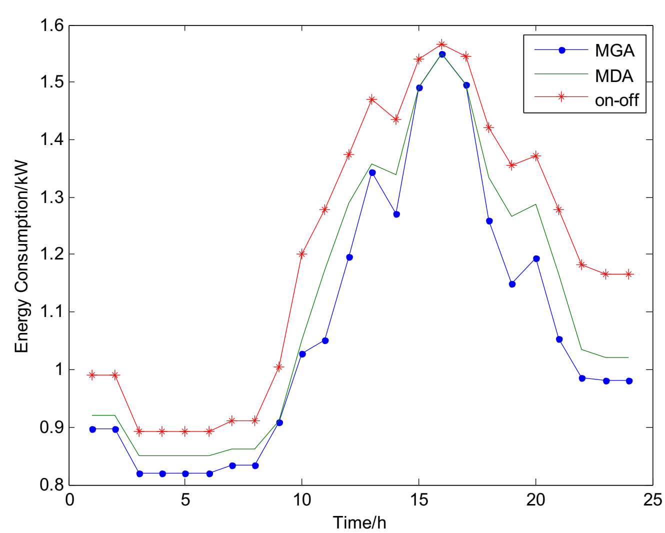

Fig. 5. Simulated energy consumption of MGA, MDA and on–off.

Table 2
Computation times of decentralized and genetic algorithms.

Time (h)	Decentralized algorithm (s)	Genetic algorithm (s)
1	7.03	664
2	6.92	646
3	6.73	643
4	6.78	655
5	6.89	633
6	6.75	673
7	6.94	671
8	6.83	680
9	6.83	699
10	6.79	705
11	6.87	682
12	6.75	659
13	6.94	649
14	6.88	662
15	7.01	634
16	6.77	692
17	6.86	687
18	6.78	649
19	6.81	703
20	6.80	667
21	6.95	676
22	6.84	642
23	6.78	681
24(0)	6.83	695

On the other hand, the global problem can be reckoned as multi-subsystem optimization which is to minimize the total costs of the whole system as well as to satisfy all the constraints from each subsystem (Pareto Optimality) [36]. If each subsystem has determined its own states and no subsystem can benefit by changing its own solution while other subsystems keep their states unchanged, these states reach their Nash Equilibrium [21,22]. The relation between Pareto optimal and Nash Equilibrium is given in the right side circle of Fig. 3.

5. Simulation and experiment results

The simulated model was built upon the measured data from lab scale pilot plant. All the coefficients of hybrid models derive from fitting the measured data. These constraints follow the system physical limits listed as in Table 1.

The cooling capacity requirement for simulation is based on a sample of one day temperature in Singapore, as shown in Fig. 4:

For the lab scale pilot plant model, energy consumption under different cooling load with decentralized optimization (MDA), centralized optimization (MGA) based on genetic algorithm and on–off control are illustrated as in Fig. 5:

The simulated results shown in Fig. 5 indicate that the energy saving effect of genetic and decentralized optimization algorithms are quite close, especially when cooling load approaches its upper bound. Numerical analysis reveals that the overall energy consumption difference between of MDA and MGA during daytime is only 3.47%, and the energy saving effect of MDA compared with on–off control is 7.16%. However, MDA saves considerable computational time; the whole algorithm only takes 6.85 s compared with MGA of 669 s, as listed in Table 2.

To verify the effect of the decentralized optimization, experimental tests are conducted on a lab scale multi-evaporator vapor compression cycle. The schematic and photo of the experimental system are illustrated in Fig. 6 and Fig. 7, respectively (Fig. 8).

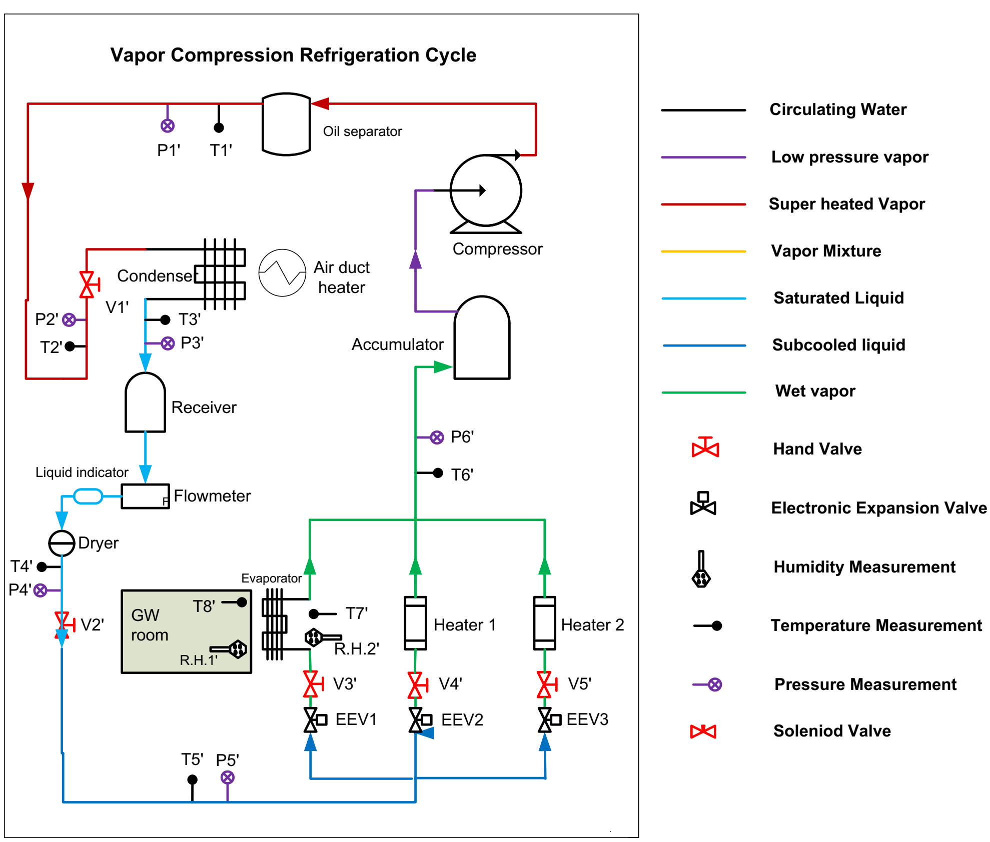

Fig. 6. Schematic of the vapor compression refrigeration system.

Fig. 7. Picture of the lab scale vapor compression refrigeration system.

The experiment system includes a semi-hermetic reciprocating compressor, an air-cooled finned-tube condenser, three electronic expansion valves and three evaporators (one air-cooled finned-tube evaporator and two electronic evaporators). One air duct heater controls the inlet air temperature of condenser for simulating outdoor condition, and the inlet air temperature of evaporator is constantly kept as 25 °C by HVAC system. The working fluid used for the system is R134a. The compressor, the condenser fan and the evaporator fan are equipped with inverters to adjust their corresponding frequencies. An air duct heater is installed in front of the condenser to control the temperature of condenser inlet air. In addition, several temperature and pressure sensors are installed for detecting state variables. To measure the mass flow rate, a flow meter with maximum 4% full scale error is used. The measurement range of the pressure transducers and the temperature transmitters are 0–16 bar and −40 °C to 200 °C, with their maximum full scale error are within ±0.3% and ±0.3 °C, respectively. The positions of these sensors are as following (refer to Fig. 6):

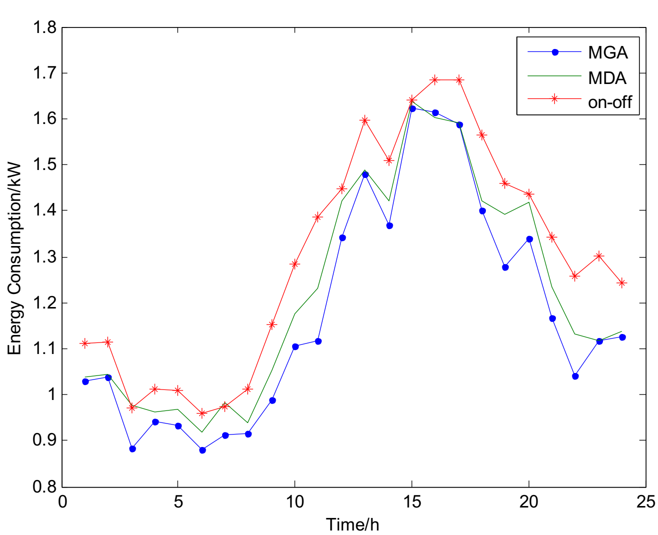

Fig. 8. Experiment results.

- refrigerant temperature and pressure at compressor outlet (T_1 and P_1);
- temperature and pressure at condenser inlet (T_2 and P_2);
- temperature and pressure at condenser outlet (T_3 and P_3);
- temperature and pressure at EEV inlet (T_5 and P_5);
- temperature and pressure at evaporator outlet (T_6 and P_6);
- mass flow rate after receiver ($\dot{m}_r$);
- relative humidity sensors at evaporator inlet and outlet (*R.H.*1, *R.H.*2).

Under the temperature scheme shown in Fig. 4, the experiment results of MDA, MGA and genetic algorithm and on–off control under are as following:

The testing results show that the energy consumptions of optimizing algorithms are smaller than that of on–off control all the time. The overall energy saving effect of MDA is 6.5% compared with on–off control, while MGA is only 3.12% better than MDA. For the time period (9–18), the difference between MGA and MDA is only 1.05%. It is also noted that energy consumption of MDA in certain periods is smaller than of MGA which may be caused by the fluctuation of incoming air temperature and humidity, both of which are unavoidable in the testing environment.

6. Conclusion

In this paper, the optimization problem for vapor compression cycle is divided into three subsystem optimization problems which subject to mechanical limitations and components interaction. Modified decentralized optimization algorithm was proposed for solving these subsystem optimization problems so that to obtain suboptimal solutions for different operating conditions. The experimental results showed that the suboptimal results calculated by MDA can reduce energy consumption compared with traditional on–off control by 6.5% for a typical day, and is larger than that of genetic algorithm by only 1.05% during the working hours. Furthermore, the average difference between simulated and experimental results for energy consumptions is 3.43%, which demonstrated the effectiveness of the proposed method. The high convergence rate of decentralized optimization suits loosely interconnected systems, an interesting topic along this direction is to study the its application in whole heating, ventilating and air conditioning systems to realize its online optimization, the problem formulation and solution procedures are currently under investigation and the findings will be reported later.

Acknowledgements

The work was funded by National Research Foundation of Singapore under the grant NRF2008EWT-CERP002-010.

Appendix A. Calculation of state variables and hybrid models

The relations between the characteristics of refrigerant are approximated and given here. ρ can be approximately calculated by a linear function of P_c and $T_{c,r,o}$

$$\rho = f_\rho(P_c, T_{c,r,o}) = a_\rho P_{c,c} + b_\rho T_{c,r,o} + c_\rho \tag{A1}$$

and the coefficients a_ρ, b_ρ, c_ρ can be obtained by curve fitting for given refrigerant.

The enthalpies of different states are completely determined by the corresponding pressure and temperature, here we will use linear functions to approximate their relation since their working ranges are not too wide, specifically:

$$H_{e,r,o} = f_{He,r,o}(P_{e,e}, T_{e,r,o}) = a_{He,r,o}P_{e,e} + b_{He,r,o}T_{e,r,o} + c_{He,r,o} \tag{A2}$$

$$H_{e,r,i} = f_{He,r,i}(P_{e,e}, T_{e,r,i}) = a_{He,r,i}P_{e,e} + b_{He,r,i}T_{e,r,i} + c_{He,r,i} \tag{A3}$$

$$H_{c,r,o} = f_{Hc,r,o}(P_{c,c}, T_{c,r,o}) = a_{Hc,r,o}P_{c,c} + b_{Hc,r,o}T_{c,r,o} + c_{Hc,r,o} \tag{A4}$$

$$H_{c,r,i} = f_{Hc,r,i}(P_{c,c}, T_{c,r,i}) = a_{Hc,r,i}P_{c,c} + b_{Hc,r,i}T_{c,r,i} + c_{Hc,r,i} \tag{A5}$$

$$\begin{aligned} H_{com,r,i} &= f_{Hcom,r,i}(P_{com,e}, T_{com,r,i}) \\ &= a_{He,r,o}P_{com,e} + b_{He,r,o}T_{com,r,i} + c_{He,r,o} \end{aligned} \tag{A6}$$

$$\begin{aligned} H_{com,r,o} &= f_{Hcom,r,o}(P_{com,c}, T_{com,r,o}) \\ &= a_{Hc,r,i}P_{com,c} + b_{Hc,r,i}T_{com,r,o} + c_{Hc,r,i} \end{aligned} \tag{A7}$$

where the coefficients $a_{He,r,o}$, $b_{He,r,o}$, $c_{He,r,o}$, $a_{Hc,r,o}$, $b_{Hc,r,o}$, $c_{Hc,r,o}$, $a_{Hc,r,i}$, $b_{Hc,r,i}$ and $c_{Hc,r,i}$ can be obtained by curve fitting for the given refrigerant.

The enthalpy differences between liquid and gas state saturated refrigerant and saturated temperature can be approximated by quadratic function of corresponding pressure, the specific forms are as following:

$$H_{e,g} = f_{He,g}(P_e) = a_{He,g}P_e^2 + b_{He,g}P_e + c_{He,g} \tag{A8}$$

$$T_{e,r,sat} = f_{Te,r,sat}(P_e) = a_{Te,r,sat}P_e^2 + b_{Te,r,sat}P_e + c_{Te,r,sat} \tag{A9}$$

$$H_{c,fg} = f_{Hc,fg}(P_c) = a_{Hc,fg}P_c^2 + b_{Hc,fg}P_c + c_{Hc,fg} \tag{A10}$$

$$T_{c,r,sat} = f_{Tc,r,sat}(P_c) = a_{Tc,r,sat}P_c^2 + b_{Tc,r,sat}P_c + c_{Tc,r,sat} \tag{A11}$$

respectively, the coefficients $a_{He,g}$, $b_{He,g}$, $c_{He,g}$, $a_{Te,r,sat}$, $b_{Te,r,sat}$, $c_{Te,r,sat}$, $a_{Hc,fg}$, $b_{Hc,fg}$, $c_{Hc,fg}$, $a_{Tc,r,sat}$, $b_{Tc,r,sat}$, $c_{Tc,r,sat}$ can be obtained by curve fitting for the given refrigerant and operating conditions. The parameters of hybrid models are given as follows:

Table A.1
Hybrid models' parameters.

Parameter	Value
$C_{e,1}$	0.7386
$C_{e,2}$	0.6820
$C_{e,3}$	0.9448
$C_{c,1}$	0.0713
$C_{c,2}$	1.4828
$C_{c,3}$	0.1302
$C_{c,4}$	0.8035
$C_{com,q,1}$	2.5138
$C_{com,q,2}$	1.2710
$C_{com,m,1}$	2.3155 e^{-3}
$C_{com,m,2}$	4.0950 e^{-4}
$C_{com,m,3}$	0.9576

Appendix B. Wolfe condition

The step length of optimization must follow Wolfe condition to tradeoff substantial reduction of objective function and time expenditure. The specific form of Wolfe condition applied to the experiment system is

$$\begin{aligned} & f(x_k + \alpha_k p_k) \le f(x_k) + 10^{-3}\alpha_k \nabla f_k^{\mathrm{T}} p_k \\ & \nabla f(x_k + \alpha_k p_k)^{\mathrm{T}} p_k \ge 0.8 \nabla f_k^{\mathrm{T}} p_k \end{aligned} \tag{B1}$$

where $p_k = -M_k^{-1}\nabla f_k$.

Appendix C. Modified Cholesky factorization

The pseudo-code of modified Cholesky factorization is given as following:

$$g = \max_{1 \le i \le n} |a_{ii}|$$

$$l = \max_{i \ne k} |a_{ik}|$$

$$M = 10^{-6} * \max(g + l, 1)$$

$$N = \max(g, \frac{l}{\sqrt{n^2 - 1}}, 10^{-6})^{0.5}$$

for $i = 1$ to n

$c_{ii} = a_{ii}$

end for

for $j = 1$ to n

for $v = 1$ to $j - 1$

$l_{jv} = c_{jv} / d_v$

end for

for $\mathrm{k} = j + 1, \quad , n$

$c_{kj} = a_{kj} - \sum_{v=1}^{j-1} l_{jv} c_{kv};$

end for

$\theta_j = 0$

if $j \le n$

then $\theta_j = \max_{j < s \le n} |c_{sj}|$

end if

$d_j = \max\left\{ |c_{jj}|, (\theta_j / N)^2, M \right\};$

if $j < n$

then for $s = j + 1$ to n

$c_{ss} = c_{ss} - c_{sj}^2 / d_j;$

end for

end if

end for

where c, a and n are elements of the modified Cholesky matrix and original matrix, and length of them, respectively.

References

[1] C. Stanfield, D. Skaves, Fundamentals of HVAC/R, Prentice Hall, Upper Saddle River, N.J., 2010.
[2] US House Hold Electricity Report, 2005.
[3] S. Building & Construction Authority, Green Building Design Guide.
[4] American Society of Heating Refrigerating and Air-Conditioning Engineers. and Knovel (Firm), 2008 ASHRAE Handbook Heating, Ventilating, and Air-conditioning Systems and Equipment (2008) (Inch-Pound ed.). Available from: http://www.knovel.com.ezlibproxy1.ntu.edu.sg/web/portal/browse/display?_EXT_KNOVEL_DISPLAY_bookid=2396.
[5] W.F. Stoecker, Industrial Refrigeration Handbook, McGraw-Hill, New York, 1998.
[6] J.-L. Lin, et al., A dynamic switching strategy for air-conditioning systems operated in light-thermal-load conditions, Applied Thermal Engineering 29 (2009) 2832–2842.
[7] X. Xiangguo, et al., Experimental study of a novel capacity control algorithm for a multi-evaporator air conditioning system, Applied Thermal Engineering 50 (2012) 975–984.
[8] S. Sanaye, H.R. Malekmohammadi, Thermal and economical optimization of air conditioning units with vapor compression refrigeration system, Applied Thermal Engineering 24 (2004) 1807–1825.
[9] J.B. Jensen, S. Skogestad, Optimal operation of simple refrigeration cycles: part I: degrees of freedom and optimality of sub-cooling, Computers & Chemical Engineering 31 (2007) 712–721.
[10] J.B. Jensen, S. Skogestad, Optimal operation of simple refrigeration cycles: part II: selection of controlled variables, Computers & Chemical Engineering 31 (2007) 1590–1601.
[11] J.B. Jensen, S. Skogestad, Steady-state operational degrees of freedom with application to refrigeration cycles, Industrial and Engineering Chemistry Research 48 (2009) 6652–6659.
[12] L.F.S. Larsen et al., A method for online steady state energy minimization, with application to refrigeration systems, in 2004 43rd IEEE Conference on Decision and Control (CDC), December 14, 2004–December 17, 2004, Nassau, Bahamas, 2004, pp. 4708–4713.
[13] E.M. Barreira, et al., Thermoeconomic analysis and optimization of residential split-type air conditioners, Applied Thermal Engineering 50 (2012) 629–636.
[14] R. Zhou, et al., The steady-state modeling and optimization of a refrigeration system for high heat flux removal, Applied Thermal Engineering 30 (2010) 2347–2356.
[15] A. Kusiak, et al., Optimization of an HVAC system with a strength multi-objective particle-swarm algorithm, Energy 36 (2011) 5935–5943.
[16] A. Kusiak, et al., Multi-objective optimization of HVAC system with an evolutionary computation algorithm, Energy 36 (2011) 2440–2449.
[17] A. Kusiak, G. Xu, Modeling and optimization of HVAC systems using a dynamic neural network, Energy 42 (2012) 241–250.
[18] K.F. Fong, et al., System optimization for HVAC energy management using the robust evolutionary algorithm, Applied Thermal Engineering 29 (2009) 2327–2334.
[19] M. Ning, M. Zaheeruddin, Neuro-optimal operation of a variable air volume HVACR system, Applied Thermal Engineering 30 (2010) 385–399.
[20] Y. Yao, J. Chen, Global optimization of a central air-conditioning system using decomposition–coordination method, Energy and Buildings 42 (2010) 570–583.
[21] G. Inalhan et al., Decentralized Optimization, with Application to Multiple Aircraft Coordination, in: Proceedings of IEEE Conference on Decision and Control, 10–13 Dec. 2002, Piscataway, NJ, USA, 2002, pp. 1147–1155.
[22] G. Inalhan, Decentralized Optimization with Independent Decision Makers, 2008.
[23] R.J. Dossat, T.J. Horan, Principles of Refrigeration, fifth ed., Prentice Hall, Upper Saddle River, N.J., 2002.
[24] D. Xudong, et al., Evaporator modeling – a hybrid approach, Applied Energy 86 (2009) 81–88.
[25] W.B. Gosney, Principles of Refrigeration, Cambridge University Press, Cambridge [Cambridgeshire], New York, 1982.
[26] C. Yiming, et al., A study on the operational stability of a refrigeration system having a variable speed compressor, International Journal of Refrigeration 31 (2008) 1368–1374.
[27] J.F. Kreider, et al., Heating and Cooling of Buildings: Design for Efficiency, McGraw-Hill, New York, 1994.
[28] D. Xudong, et al., A hybrid condenser model for real-time applications in performance monitoring, control and optimization, Energy Conversion and Management 50 (2009) 1513–1521.
[29] X. Ding et al., A hybrid modeling for the real-time control and optimization of compressors, in 2009 4th IEEE Conference on Industrial Electronics and Applications, ICIEA 2009, May 25, 2009–May 27, 2009, Xi'an, China, 2009, pp. 3256–3261.
[30] C.P. Arora, Refrigeration and Air Conditioning, second ed., Tata McGraw-Hill, New Delhi, 2000.
[31] B.P. Rasmussen, Dynamic modeling and advanced control of air conditioning and refrigeration systems, Ph.D. 3202157, University of Illinois at Urbana-Champaign, United States – Illinois, 2005.
[32] S.L. Dixon, C.A. Hall, Fluid Mechanics and Thermodynamics of Turbomachinery, sixth ed., Butterworth–Heinemann/Elsevier, Burlington, MA, 2010.
[33] J. Nocedal, S.J. Wright, Numerical Optimization, second ed., Springer, New York, 2006.
[34] D.P. Bertsekas, Convex Optimization Theory, Athena Scientific, Belmont, Mass., 2009.
[35] G. Inalhan, Decentralized Optimization across Independent Decision Makers with Incomplete Models, Ph.D. 3145523, Stanford University, United States – California, 2004.
[36] T.J. Webster, Introduction to Game Theory in Business and Economics, M.E. Sharpe, Armonk, N.Y., 2009.
[37] S.W. Data, http://freemeteo.com/default.asp?pid=20&gid=1880252&la=1&sid=486980&md=0&ndate=16/06/2011&lc=5.